Electronic Supplementary Information

Amphiphilic PVDF-*g*-POEM double comb copolymers based solid-state electrolyte for EDLC applications: Electrochemical and electrical properties study

Uoon Chul Baek[a], Da Hye Sim[b] and Jung Tae Park*[,a]

[a] Department of Integrated Display Engineering, Yonsei University,
50 Yonsei-ro, Seodaemun-gu, Seoul 03722, Republic of Korea
[b] Department of Chemical and Biomolecular Engineering, Yonsei University,
50 Yonsei-ro, Seodaemun-gu, Seoul 03722, Republic of Korea

* To whom correspondence should be addressed.

Tel: +82-2-2123-5828

E-mail: jtpark25@yonsei.ac.kr (J.T. Park)

1. Materials and Experimental method

Material

The Polyvinylidenefluoride (PVDF; Solvay 6010) was purchased from Solvay Specialty Polymers (Bollate, Italy). Carbon paper (Spectracarb 2050A-1550) was purchased from Nara Cell Tech (Seoul, Republic of Korea). CuCl (>99.995%), poly(ethylene glycol) methyl ether methacrylate (POEM; $M_n \sim 500$ g / mol), and activated carbon were purchased from Sigma-Aldrich (St. Louis, MO, USA). Carbon black (Super P), 4,40-dimethyl-2,20-dipyridyl (DMDP) and LiTFSI (99%) were purchased from Thermo Fisher Scientific (Waltham, MA, USA). N-Methyl-2-pyrrolidone (NMP), N, N-dimethylformamide (DMF), and methanol were obtained from J. T. Baker (Phillipsburg, NJ, USA). Deionized water (>18 MΩ m) was obtained using a water purification system manufactured by MilliporeSigma (Burlington, MA, USA).

Experimental Methods

Synthesis of amphiphilic PVDF-*g*-POEM double comb copolymers

The double comb polymer was synthesized based on the reported ATRP mechanism with adjustments.[1] PVDF (5 g) was dissolved in 50 mL NMP in a 250 mL round-bottom flask. After stirring until homogeneous, 0.04 g CuCl catalyst was added, followed by stirring for 1 h, and then 0.23 g DMDP ligand was added, followed by further stirring for 1 h. Subsequently, after purging with N_2 gas, POEM was added, and the flask was placed in a 90 °C oil bath for 24 h. The sample was then precipitated in methanol and washed four times. Subsequently, the sample was dried in a 50 °C vacuum oven.

Preparation of the solid-state electrolyte

The solid-state electrolyte was prepared by casting. Amphiphilic PVDF-*g*-POEM double comb copolymers or hydrophobic PVDF (0.1 g) were dissolved in 1 mL DMF. After complete dissolution of the polymer, different amounts of LiTFSI were added and dissolution proceeded over 3 h. The obtained solution was cast onto a glass substrate under atmospheric pressure and room temperature to form a uniform solid-state electrolyte.

Preparation of the EDLC Cells

Activated carbon, Super P, and PVDF (8:1:1) were mixed homogenously in NMP to obtain a uniform slurry. The slurry was coated onto carbon paper using the doctor-blade technique and dried at 80 °C, with an average mass loading of 7 mg cm^{-2} of the active material. The solid-state electrolytes were sandwiched as separators and were additionally cast directly onto the coated material of the electrode. These cells were assembled symmetrically and then dried at 80 °C to produce EDLC cells. The configuration of the assembled supercapacitor is shown in Scheme 1(b).

2. Characterization

^{1}H-NMR spectroscopy was conducted using high-resolution 600 MHz spectrometers (AVANCE 600, Bruker, Billerica, MA, USA) with DMF-d6 as the solvent. Signals corresponding to PVDF (head-to-head (hh) and head-to-tail (ht)), O-CH_x, and POEM (PEO) are observed in the ^{1}H-NMR spectra of PVDF-*g*-POEM. The moles and mass of POEM within the copolymer are calculated using equations S1 and S2 [2]:

$$\varphi_{m(POEM)} = (1/37(I_c + I_d + I_e))/(1/37(I_c + I_d + I_e) + 1/2(I_{a(hh)} + I_{a(ht)})) \quad \text{(S1)}$$

$$\varphi_{w(POEM)} = \varphi_{(m(POEM)} \times M_{POEM}/((\varphi_{(m(POEM)} \times M_{POEM}) + (1 - \varphi_{m(POEM)}) \times M_{(\ PVDF(unit))}) \quad \text{(S2)}$$

where $\varphi_{m(POEM)}$ and $\varphi_{w(POEM)}$ are the mole and weight fractions of POEM, respectively, I_x is the area under the corresponding signal, and M_{POEM} and M_{PVDF}(unit) are the molecular weights of POEM and the PVDF monomer, respectively. Thermogravimetric analysis (TGA) was conducted under air atmosphere (510 °C min^{-1}) using a Discovery TGA (TA Instruments, Hüllhorst, Germany). All samples were heated from room temperature 25 °C to 600 °C. The thermal behavior of the polymer was characterized under N_2 gas using a DSC-Q1000 (TA Instruments) operating at a heating rate of 10 °C min^{-1}. All samples were heated from −80 °C to 200 °C. FT-IR spectroscopy was performed using an Excalibur Series FT-IR (Digilab, Hopkinton, MA, USA) spectrometer in the frequency range 4000–600 cm^{-1} using attenuated total reflectance with resolution of 2 cm^{-1}. The ionic conductivity was measured via a two-probe method using two stainless-steel blocking electrodes and a potentiostat in the frequency range 10^{-1} MHz with a sinusoidal amplitude of 10 mV. The sample conductivities are calculated using the bulk electrolyte resistances R (Ω) found in the complex impedances using the following equation:

$$\sigma = d/AR \qquad \text{(S3)}$$

where R, A, and d represent the electrical resistance of the electrolyte (Ω), area of the stainless-steel electrodes (cm^2), and distance between the two stainless-steel electrodes (cm), respectively. The electrical properties of the EDLCs were investigated using a VSP potentiostat (BioLogic, Seyssinet-Pariset, France) equipped with a frequency analyzer. For the performance of the supercapacitor, the capacitance is often calculated in specific capacitance (Cs, F g^{-1}), which is calculated from the cyclic voltammograms using equation (S4):

$$Cs = \int I \, \mathrm{d}V / 2mv\Delta V \qquad \text{(S4)}$$

where I (A) is current, m (g) is the mass of the active material, v (V s^{-1}) is the scan rate, and ΔV (V) is the potential range of the cyclic voltammograms. Additionally, galvanostatic charge-discharge (GCD) curves are used to calculate the capacitance (Cs) from the discharge time at constant current using equation (S5):

$$Cs = I_d \Delta t / m\Delta V \qquad \text{(S5)}$$

where I_d (A) is the discharge current, Δt (s) is the discharge time, m (g) is the mass loading of the active material, and ΔV (V) is the potential window. For an energy storage system, the energy and power parameters, energy density (E, Wh kg^{-1}) and power density (P, W kg^{-1}), are calculated using equations (S6) and (S7):

$$E = (1/2*3.6)C\Delta V^2 \qquad \text{(S6)}$$

$$P = 3600\, E/\Delta t \qquad \text{(S7)}$$

Where C (F g^{-1}) is specific capacitance, ΔV is potential window, and Δt (s) is the discharge time. Microphase-separated structures were observed using a spherical-aberration-corrected transmission electron microscope (JEM-ARM 200F, JEOL). Sample preparation was as follows: 0.01 g synthesized copolymer was dissolved in 1 mL DMF (containing a few drops of HCl/H_2O). This polymer solution was deposited on an ultrathin carbon-coated surface of a Cu grid. The crystal morphology was determined using high-resolution XRD (SmartLab, Rigaku, Tokyo, Japan) in the 2θ range 10°–50° at a scan rate of 3° min^{-1} using Cu Kα radiation. Transmission SAXS was performed using the 4C SAXSII beamline at the Pohang Light

Source, Republic of Korea, with a sample-to-detector distance of 4 m, and a beam size of 0.023 × 0.300 mm^2. A 2D charge-coupled device detector (SX165, Rayonix, Evanston, IL, USA) was used to collect the scattered X-rays within an exposure time of 10 s.

3. Supplementary Results

Table S1. T_m, T_c and χ_c of the hydrophobic PVDF and amphiphilic PVDF-*g*-POEM double comb copolymer. [a,b,c]

	[a]T_m (°C)	[b]ΔH_f (J g^{-1})	[c]χ_c (%)
PVDF	170.2	51.02	48.7
PVDF-*g*-POEM	169.5, 172.2	26.26	26.3

[a] T_m is melting temperature.

[b] H_f is enthalpy of fusion

[c] χ_c is crystallinity.

Melting points (T_m), enthalpy of fusion (ΔHf) and degree of crystallinity (χ_c) of the hydrophobic PVDF and amphiphilic PVDF-*g*-POEM double comb copolymer POEM obtained from DSC thermogram. The degree of crystallinity (χ_c) of PVDF is calculated using equation S8:

$$\chi_c = \Delta Hf/\Delta H^*f \qquad \text{(S8)}$$

where ΔHf is the sample enthalpy of fusion (J g^{-1}) and ΔH^*f is the heat of fusion of perfectly crystalline PVDF (104.5 J g^{-1}).[3]

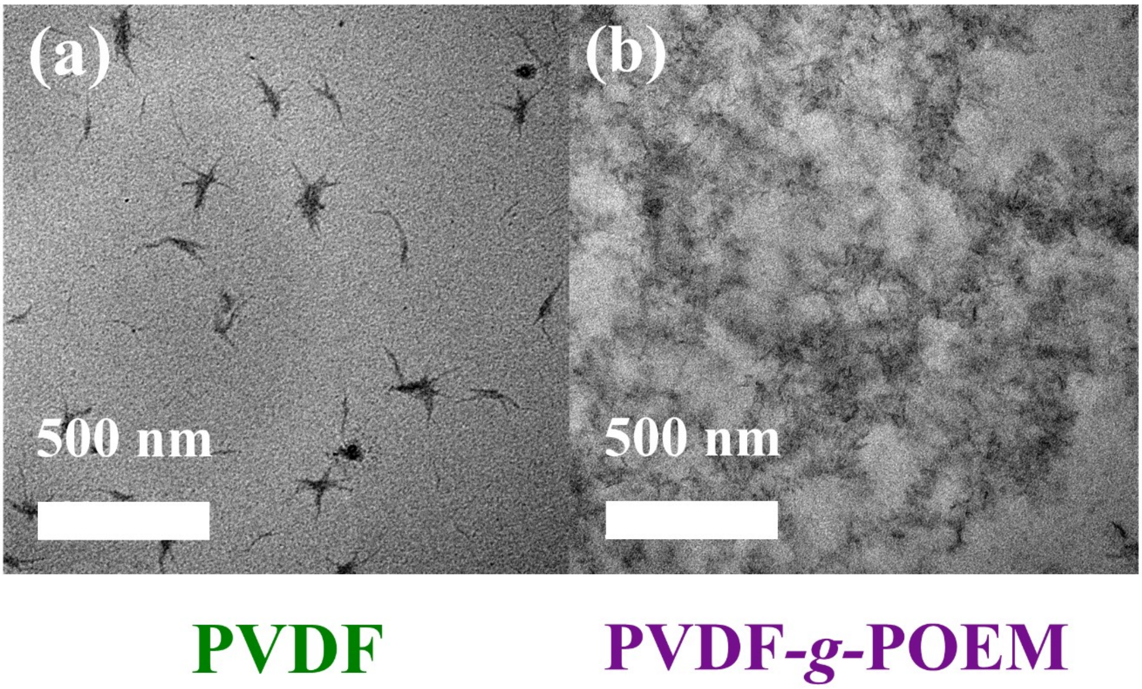

Figure S1. TEM images of (a) hydrophobic PVDF, (b) amphiphilic PVDF-*g*-POEM double comb copolymer prepared from NMP/H_2O/HCl.

The morphology of the polymer is characterized using TEM images (Figure S1). Compared to those of hydrophobic PVDF, the amphiphilic PVDF-*g*-POEM double comb copolymer domains reveal the phase separation of the polymer. The hydrophobic PVDF domains appear as darker regions compared to those of the hydrophilic POEM domains, due to the higher electron densities of the fluorine atoms. The well-connected, well-aligned POEM channels of PVDF-*g*-POEM effectively form unique pathways for ionic conductivity. For further analysis of the polymer matrix as an electrolyte, the polymer samples were dissolved in DMF to prepare solid-state electrolytes by adding different weight% concentrations of LiTFSI with respect to the host polymer.

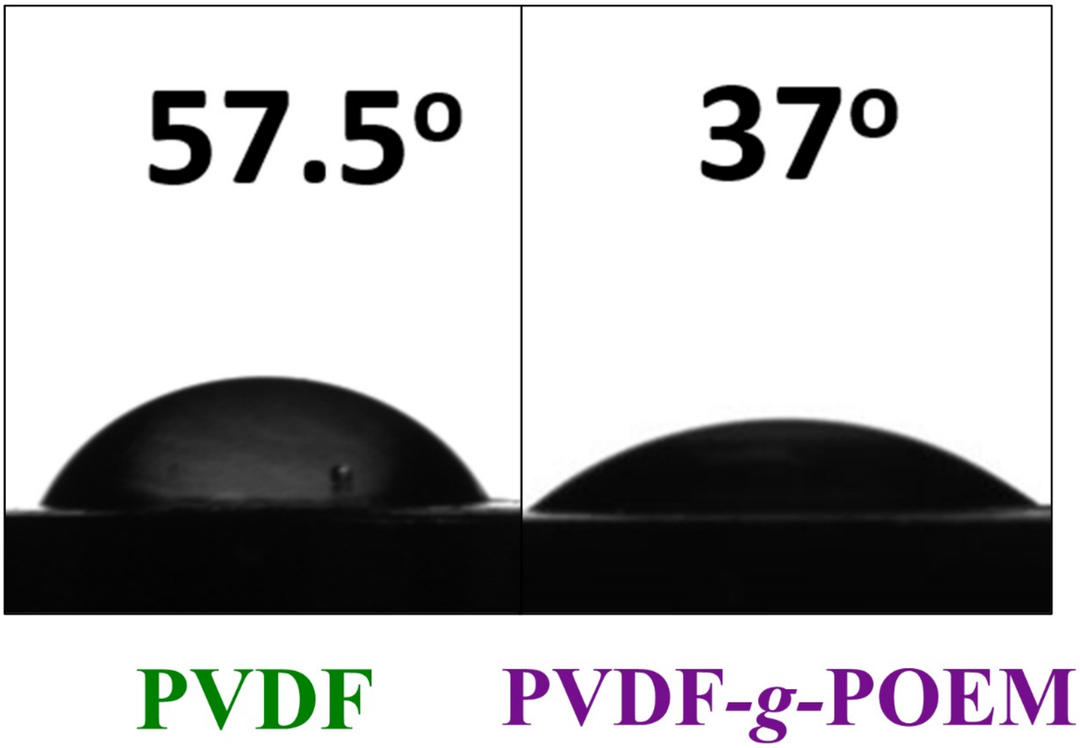

Figure S2. Contact angle measurement of hydrophobic PVDF (left) and amphiphilic PVDF-*g*-POEM double comb copolymer (right).

The contact angle of the amphiphilic PVDF-*g*-POEM double comb copolymer-based solid-state electrolyte is lower (57.5°, Figure S2) than that of the hydrophobic PVDF electrolyte (37°) due to the higher hydrophilicity of the POEM polymer. This improved wettability increases the accessibility of the electrolyte to the electrode surface, resulting in improved capacitance properties.

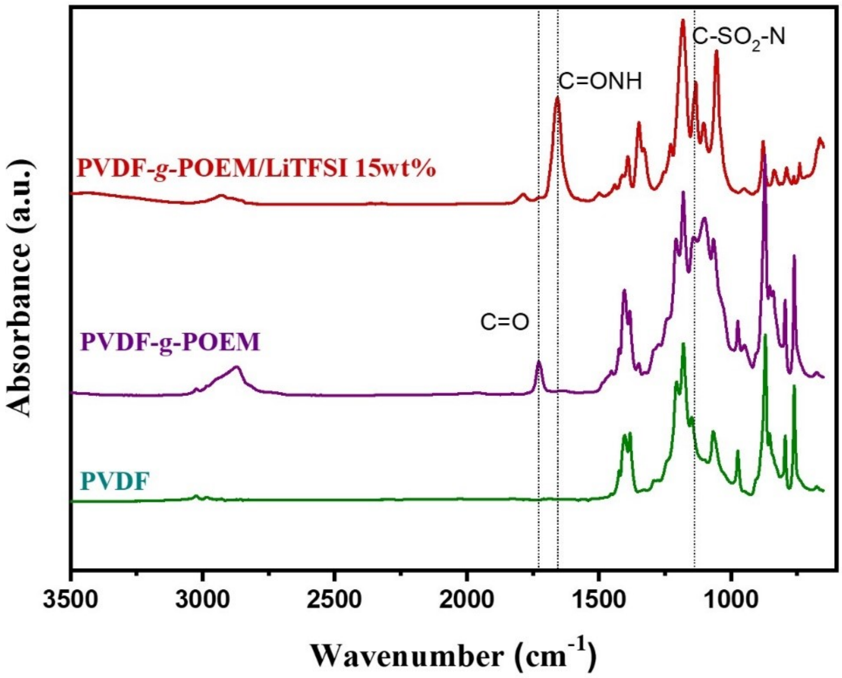

Figure S3. FT-IR spectra of solid-state electrolytes prepared from hydrophobic PVDF and amphiphilic PVDF-*g*-POEM double comb copolymer and PVDF-*g*-POEM/LiTFSI 15wt%.

The coordinative interactions between the Li salt and the solid-state electrolyte based on amphiphilic PVDF-*g*-POEM double comb copolymer were characterized using FT-IR spectroscopy, as shown in Figure S3. By introducing the LiTFSI, the peaks assigned to the C=O stretching mode of PVDF-*g*-POEM are shifted to lower wavenumbers of 1727 and 1724.5 cm^{-1}, respectively, indicating coordinative interactions between the lithium ions and carbonyl oxygens, while residual DMF peaks are observed at 1783 cm^{-1}. This strongly suggests Li$^+$ interaction with the carbonyl groups of the POEM chains. Additionally, the C–SO$_2$–N bonding vibration of TFSI$^-$, which is generally observed at 1326.5 cm^{-1} in LiTFSI, is shifted to 1330.5 cm^{-1} in the spectra of the solid-state electrolyte, suggesting that electrostatic attraction between these anions and the polymers also occurs.

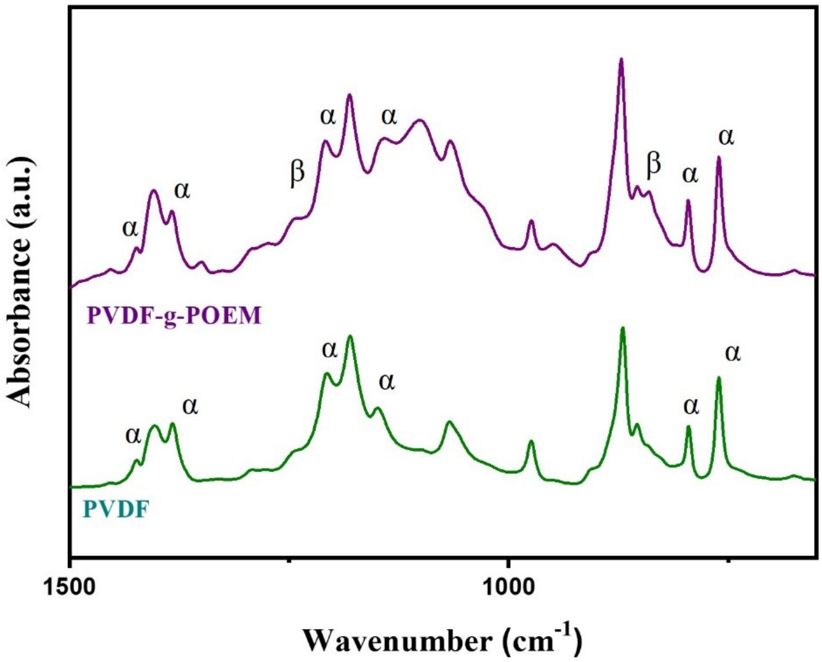

Figure S4. Phase assignments of hydrophobic PVDF and amphiphilic PVDF-*g*-POEM double comb copolymer in FT-IR spectra.

The known α, β, of PVDF are analyzed using FT-IR spectroscopy (Figure S4), where α (TGTG′, form II) and β (TTTT, form I) are observed. The α phase of PVDF is indicated by the peaks at 1423, 1383, 1209, 1149, 975, 854, 795, and 763 cm^{-1}, whereas the β phase is indicated by the peaks at 1431 and 1275 cm^{-1}.[4] The amphiphilic PVDF-*g*-POEM double comb copolymers show an increase in β phase formation, presumably due to the solvent effect of NMP and the copolymer contribution upon polymer synthesis.[5–7] From the phase change within the polymer, amphiphilic PVDF-*g*-POEM double comb copolymer contains an increased ratio of the β phase, yielding a higher melting point.[8] Furthermore, for amphiphilic PVDF-*g*-POEM double comb copolymer, the increased β phases affect the crystallinities of the polymers. The lower crystallinities enhance the performances of the solid-state electrolytes.[9,10]

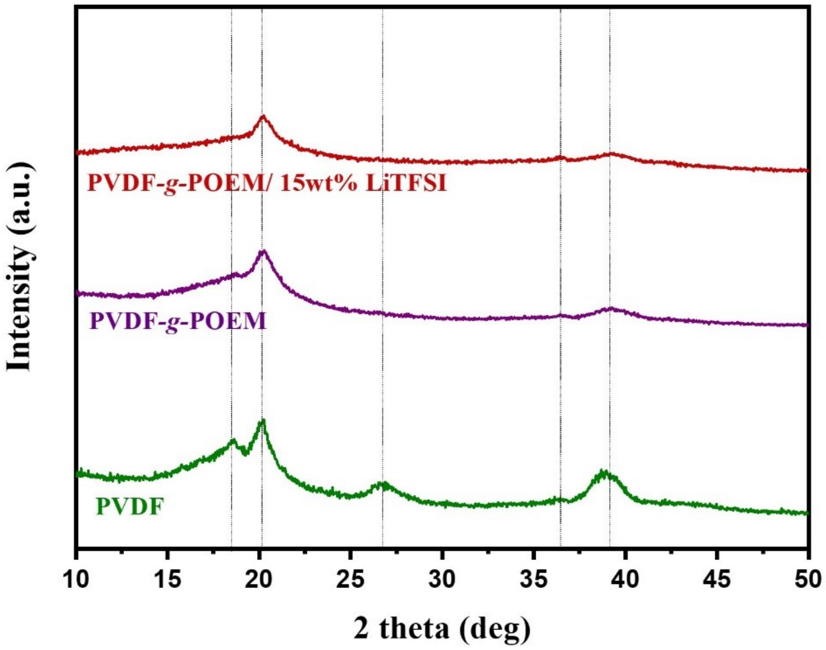

Figure S5. XRD of membranes prepared with hydrophobic PVDF and amphiphilic PVDF-*g*-POEM double comb copolymer, PVDF-*g*-POEM /LiTFSI 15wt%.

XRD was used to study the synthesized solid-state electrolyte. Figure S5 shows dominant peaks at 2θ = 18.58°, 26.83°, and 38.63°, which correspond to the α phase of the PVDF, and the peak at 2θ = 20.26° corresponds to the β phase of PVDF.[4] These peaks indicate the semi-crystalline nature of the polymer, wherein the crystalline regions are mixed with the amorphous phase. The α phase-related peaks of the double comb copolymer are diminished, whereas the β phase-related peak is slightly dominant. This phenomenon was observed for various PVDF due to various factors, such as the specific interaction of the polymer with the copolymer, solvent, and thermal treatment.[11] The broadening of the peak confirms an increase in the amorphous region which indicates enhanced ionic conductivity, attributed to the availability of free space for ionic motion.

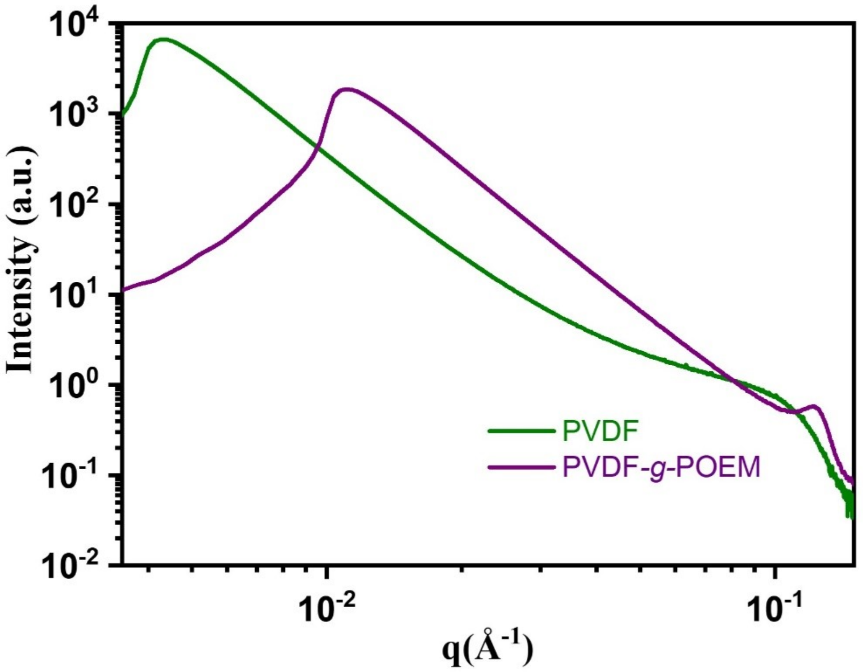

Figure S6. SAXS images of hydrophobic PVDF and amphiphilic PVDF-*g*-POEM double comb copolymer and its *q* vector position for d-spacing calculation.

Additionally, the SAXS analysis, which reveals the overall structure of the polymer, is shown in Figure S6, based on equation (S9):

$$q = 2\pi/d \qquad \text{(S9)}$$

where q is the scattering vector q (Å^{-1}) and d is the d-spacing of the polymer. The increased d-spacing is attributed to the fusion of the POEM side chains to the PVDF chains, which impedes close crystal stacking. Thus, PVDF-*g*-POEM provides an improved matrix for a solid-state electrolyte, with the less-tightly packed matrix resulting in superior ionic conductivity. The calculated d-spacing of the neat PVDF is 5.1 nm, whereas PVDF-*g*-POEM exhibits a d-spacing of 6.2 nm.

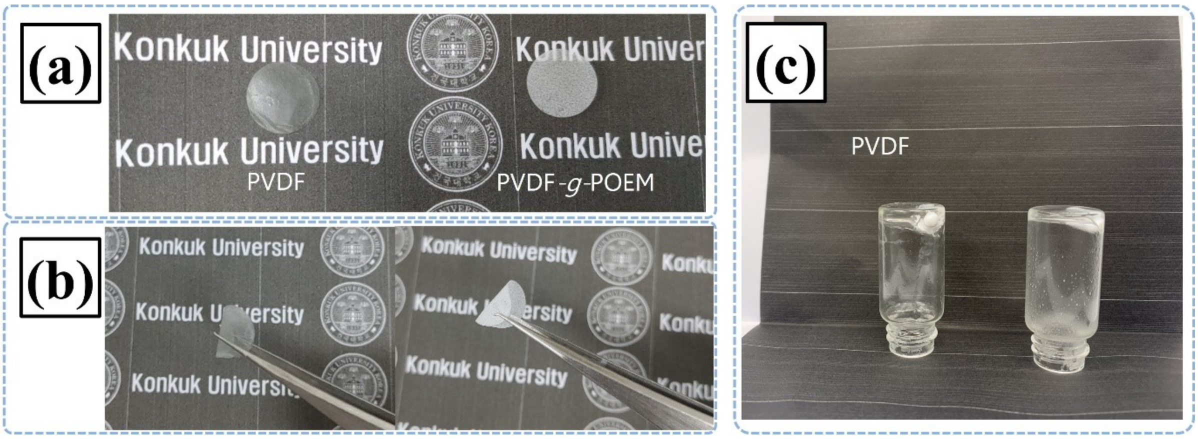

Figure S7. (a) Photographic images of the (a) hydrophobic PVDF and amphiphilic PVDF-*g*-POEM double comb copolymer based solid-state electrolyte (b) folded solid-state electrolytes held with tweezers (c) the solid-state electrolytes plasticized in DMF.

While both hydrophobic PVDF and amphiphilic PVDF-*g*-POEM double comb copolymer based electrolyte showed gel state when plasticized by DMF. When dried to form solid-state membrane states, both shows solid but stable mechanical states.

Table S2. Ionic conductivity and activation energy of solid-state electrolyte based on PVDF/LiTFSI, PVDF-*g*-POEM/LiTFSI.

LITFSI content (wt/wt%)		0%	10%	15%	33%	75%
Ionic conductivity σ (Scm^{-1})	PVDF	7.87×10^{-7}	5.66×10^{-5}	8.32×10^{-5}	7.12×10^{-5}	1.25×10^{-5}
	PVDF-*g*-POEM	9.19×10^{-7}	6.23×10^{-5}	9.23×10^{-5}	5.33×10^{-5}	2.16×10^{-5}

In polymer electrolytes, ions must overcome energetic barriers associated with polymer chain motion and interactions between ions and the polymer matrix. This process follows Arrhenius-type behavior, where ionic conductivity σ (s cm^{-1}) typically increases exponentially with increasing temperature. Thus, activation energy Ea (eV) can be derived using the Arrhenius equation (S10):

$$\sigma = A\mathrm{e}^{(-Ea/kT)} \qquad \text{(S10)}$$

where Boltzmann constant k and T (K) is used to calculate activation energy from the Arrhenius plot.

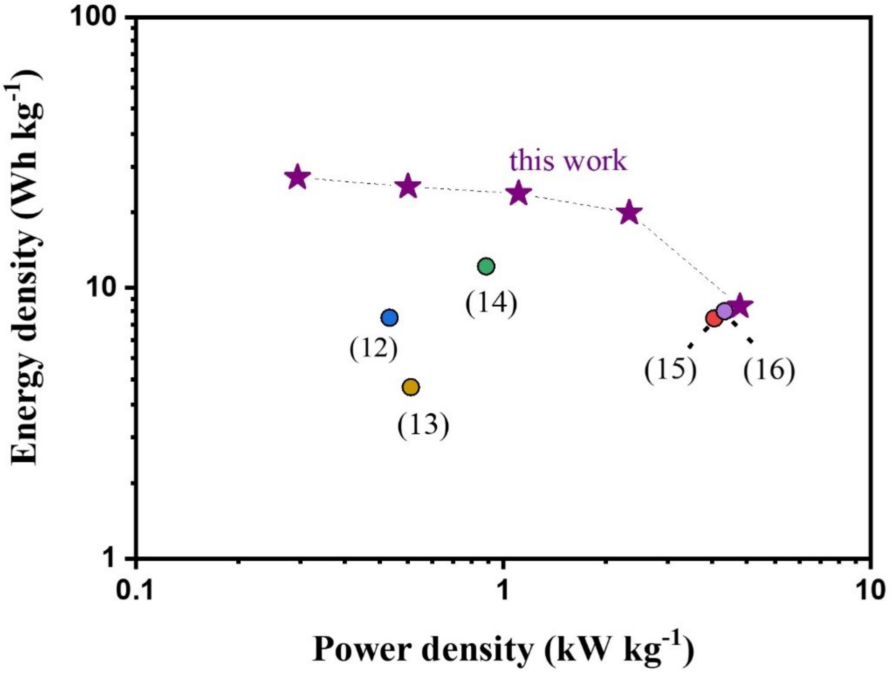

Figure S8. Ragone plot of the fabricated cell prepared with PVDF-*g*-POEM /LiTFSI 15wt%

Figure S8 shows Ragone plot calculated from Equation S6 and S7. Table S3 shows comparison of power and energy densities of the EDLC with amphiphilic PVDF-*g*-POEM double comb copolymer based solid-state electrolyte provided with this work. Our work showed the highest power density of 0.275 kW Kg^{-1}, with energy density of 25.59 Wh Kg^{-1}, indicating outstanding performance of amphiphilic PVDF-*g*-POEM double comb copolymer based solid-state electrolyte compared to hydrophobic PVDF based polymer electrolytes.[12-16]

Table S3. Comparison of the specific capacitance, highest conductivity, cycle number and stability, power and energy densities between this study and other works.

Electrolyte	Specific Capacitance	Highest Conductivity	Cycle Number/ Stability	Power Density	Energy Density	Ref.
	(F g^{-1})	(mS cm^{-2})	-	(kW Kg^{-1})	(Wh Kg^{-1})	
PVDF-*g*-POEM /LiTFSI 15wt%	38.07	9.23	8000/ 85%	0.275	25.59	This work
PVdF-HFP/0.5M NaBF4/EC:PC/Acetone/Methylene Blue	114	2.3	10000/ 64%	0.49	7.76	12
PVdF-HFP/TEABF4/EC:PC/SiO2	45.3	8.2	3000/ 90%	0.56	4.3	13
PVdF-HFP/EMITf/ Al(Tf)3/DMF	323.9	0.8	15000/ 100%	0.9	12	14
PVdF-HFP/BMIMTFSI/EC/DMF	78.8	8.18	3000/ 88.9%	3.75	7.71	15
PVdF-HFP/LiTFSI/ SN	57	2	3500/ 80%	4	8.2	16

Table S4. Specific capacitance in different scan rates with cell prepared with PVDF-*g*-POEM /LiTFSI 15wt% in CV.

Scan rate (mV s^{-1})	Specific capacitance (F g^{-1})
500	9.7
200	15.82
100	19.79
50	23.2
20	14.76
10	31.27
5	36.98

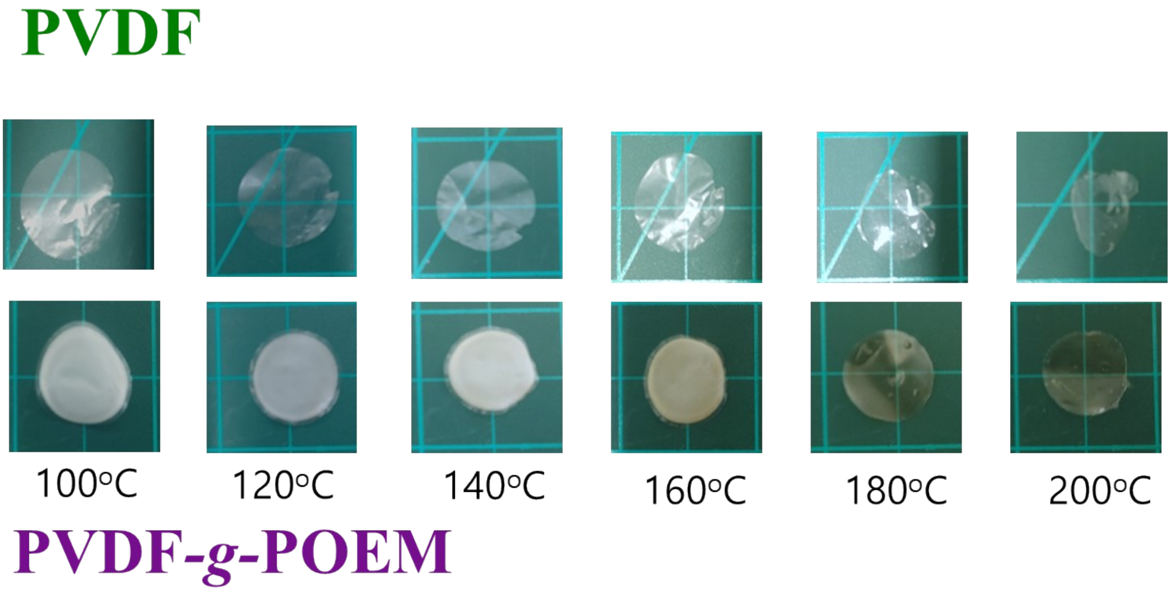

Figure S9. Photographic images of hydrophobic PVDF and amphiphilic PVDF-*g*-POEM double comb copolymer based solid-state electrolytes exposed at high Temperatures.

The amphiphilic PVDF-*g*-POEM double comb copolymer based solid-state electrolytes showed stability at high temperature showing high thermal stability

4. References

1. J. F. Hester, P. Banerjee, Y.-Y. Won, A. Akthakul, M. H. Acar and A. M. Mayes, ATRP of amphiphilic graft copolymers based on PVDF and their use as membrane additives, *Macromolecules*, 2002, **35**, 7652–7661

2. M. R. Moghareh Abed, S. C. Kumbharkar, A. M. Groth and K. Li, Economical production of PVDF-*g*-POEM for use as a blend in preparation of PVDF-based hydrophilic hollow fibre membranes, *Sep. Purif. Technol.*, 2013, **106**, 47–55

3. S. Lanceros-Méndez, J. F. Mano, A. M. Costa and V. H. Schmidt, FTIR and DSC studies of mechanically deformed β-PVDF films, *J. Macromol. Sci. Phys.*, 2001, **40**, 517-527.

4. X. Cai, T. Lei, D. Sun and L. Lin, A critical analysis of the α, β and γ phases in poly(vinylidene fluoride) using FTIR, *RSC Adv.*, 2017, **7**, 15382-15389.

5. Z. J. Huang, J. Jiang, G. Xue and D. S. Zhou, β-Phase crystallization of poly(vinylidene fluoride) in poly(vinylidene fluoride)/poly(ethyl methacrylate) blends, *Chin. J. Polym. Sci.*, 2019, **37**, 94-100.

6. S. Janakiraman, A. Surendran, S. Ghosh, S. Anandhan and A. Venimadhav, Electroactive poly(vinylidene fluoride) separator for sodium ion battery with high coulombic efficiency, *Solid State Ionics*, 2016, **292**, 130-135.

7. L. Ruan, X. Yao, Y. Chang, L. Zhou, G. Qin and X. Zhang, Properties and applications of the β phase poly(vinylidene fluoride), *Polymers (Basel)*, 2018, **10**, 228

8. B. Jaleh, S. Sodagar, A. Momeni and A. Jabbari, Nanodiamond particles/PVDF nanocomposite flexible films: thermal, mechanical and physical properties, *Mater. Res. Express*, 2016, **3**, 085028.

9. R. J. Sengwa and P. Dhatarwal, Predominantly chain segmental relaxation dependent ionic conductivity of multiphase semicrystalline PVDF/PEO/$LiClO_4$ solid polymer electrolytes, *Electrochim. Acta*, 2020, **338**, 135890.

10. M. Tripathi, S. M. Bobade and A. Kumar, Preparation of polyvinylidene fluoride-*co*-hexafluoropropylene-based polymer gel electrolyte and its performance evaluation for application in EDLCs, *Bull. Mater. Sci.*, 2019, **42**, 27.

11. N. Govinna, I. Sadeghi, A. Asatekin and P. Cebe, Thermal properties and structure of electrospun blends of PVDF with a fluorinated copolymer, J. *Polym. Sci. Part B Polym. Phys.*, 2019, *57*, 312-322.

12. Singh M. K., Sharma A. K. and Chaurasia S. K., Enhanced energy density of quasi-solid-state supercapacitor based on activated carbon electrode derived from honeycomb and gel polymer electrolyte with redox-additive methylene blue, *Energy Storage*, 2023, **6 (1)**, e514.

13. Mukta Tripathi, B. K. Dwivedi, Y. Kumar, S. M. Bobade and A. Kumar, Synthesis and performance assessment of silica dispersed nano-composite polymer gel electrolyte for high-performance solid-state supercapacitors, *J. Electroanal. Chem.*, 2024, **948**, 117797.

14. J. Liu, Z. Khanam, S. Ahmed, H. Wang, T. Wang and S. Song, A study of low-temperature solid-state supercapacitors based on Al-ion conducting polymer electrolyte and graphene electrodes, *J. Power Sources*, 2021, **488**, 229461

15. C.-C. Yang, H.-Y. Lin, A. Kumar, B. Pattanayak, H.-Y. Tsai, T. Winie and T.-Y. Tseng, Flexible solid-like electrolytes with ultrahigh conductivity and their applications in all-solid-state supercapacitors, *RSC Adv.*, 2018, **8**, 30239–30247.

16. M. K. Singh, M. Suleman, Y. Kumar and S. A. Hashmi, A novel configuration of electrical double layer capacitor with plastic crystal based gel polymer electrolyte and graphene nano-platelets as electrodes: a high rate performance, *Energy*, 2015, **80**, 465–473.